Mechanical Properties of 3D Printed Parts and Discovering Zinc Fused deposition modeling

Marlon Leong

Bachelor of Engineering (Honours)
Major Mechanical Engineering

Department of Mechanical Engineering
Macquarie University

November 6, 2017

Supervisors: Doctor Wei Xu and Professor Candace Lang

ACKNOWLEDGEMENTS

I would like to acknowledge, my parents for enduring support throughout my bachelor's degree. To my closest friend and brother Lyndon whom has helped me at any notice. To my Academic Supervisors Professor Candace Lang, Doctor Wei Xu and unit conveyor Raheel Hasmi for assisting me in restarting and continuing my thesis after an abrupt academic deferral. To the crucial taskmasters Walther Adendorff, Wendy Tao and Mynga Nguyen for support and designation for facility resources. To these people I greatly appreciate due to the difficulty of this project.

STATEMENT OF CANDIDATE

I, Marlon Leong, declare that this report, submitted as part of the requirement for the award of Bachelor of Engineering in the Department of Mechanical Engineering, Macquarie University, is entirely my own work unless otherwise referenced or acknowledged. This document has not been submitted for qualification or assessment an any academic institution.

Student's Name: Marlon Leong

Student's Signature: 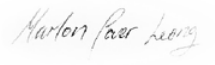

Date: 6/11/2017

Noteworthy

Initially the thesis began earlier in the year as a study focused on Fused Deposition Modeling (FDM) printing of Polylactic acid (PLA), Acrylonitrile-Butadiene-Styrene (ABS) plastic and selective laser sintering (SLS) $Ti_{64}Al_4V$ alloy materials. The study goal was to juxtapose emerging 3d printing manufacturing methods versus traditional methods. Unfortunately, this was abruptly interrupted to which I could not control. Time passed and technologies changed. The idea of $Ti_{64}Al_4V$ was dropped due to time constraints and costings. The focus now is additionally on FDM printing of Zinc and variant alloys. Thomas Yuen is working in conjunction of this Zinc alloy FDM project. Yuen's thesis, aims at developing a suitable zinc magnesium metal alloy to which we trifle as Magzinc. This was incited week 3 (mid-August) and development is still underway. The study is now aimed at comparing methods of manufacture but also provoking the method of Zinc metals FDM, with the idea of creating a cheaper metal 3d printing alternative then selective laser sintering, SLS, with applications for Biomedical and electronics industries.

ABSTRACT

3D printing is becoming a common method of additive manufacturing complex parts for assembly or final net-shape items. The final 3d-printed artefact is to be investigated and compared against traditional methods of manufacturing (injection molding). To investigate the effect of the 3d printing parameters, layer size, temperature, print head speed and filament material. This paper will investigate and develop novel direct Zinc metal FDM for possible applications such as Biomedical and electronics tracing. The novel metal FDM will focus on pure zinc (99.99%) with future developments for zinc magnesium alloys. The purpose of this novel FDM is to produce biocompatible complex shapes for vivo use and for electronics as traces for circuitry.

Contents

List of Figures

List of Tables

1 Introduction

Additive manufacturing, AM, development began in the early 1990's [1] and is now economically viable for commercial and retail users. This is mainly attributed to the patent expiry on FDM 3d printing, allowing 3rd party and opensource FDM developments for mass commercialisation. Developments have been made that allow for diverse printing applications, a broader spectrum of printing materials and many developing printing techniques. Due to the increasingly ubiquitous nature of 3D printing technology, an increase in demand for analysis of both material and mechanical properties has emerged. An important emerging field is for $Ti_{64}Al_4V$ SLS printing for biomedical implants, which is price and time expensive usually requiring post operation removal. Zinc magnesium alloys are investigated to be vivo biocompatible and decomposable. Therefor creating a pursuit for alternative technologies and the rise of the development of metal Zinc magnesium alloy FDM 3D printing.

1.1 Project Goal

The project aims at evaluating of the limitations of 3D printing (specifically FDM) regarding the printing parameters. These limitations will aid in developing a novel Zinc metal FDM 3d printing. Ultimately this paper is aimed at providing a new method of 3d printing biomedical implants using a Zinc Magnesium alloy filament (Magzinc). Zinc magnesium alloys have been shown to have biomedically compatible with the ability to be dissolved overtime or permanently (PLA coatings) [2]. This allows for non-post operation transplants such as titanium screws. The finale is to produce a Zinc print of a lumbar vertebra, which would show the ultimate success of the research.

The difficulty of the project varies, thermoplastic FDM is already a wide spread field which will make the task easier. Zinc FDM is undeveloped and will be challenging. The Zinc filament may involve a magnesium 0~5% content which will be referenced to as Magzinc. Methods for the production of zinc (non-alloy) and Magzinc filaments will have to be investigated. The paper will also highlight the crucial differences between establish thermoplastic FDM and metal (zinc) FDM.

To help achieve these goals a top down feedback loop approach was conducted, see Figure 1. This management approach naturally occurred as the project progressed. Concepts, thoughts and brain storming was conduct throughout the project with the supervision of Doctor Xu, Professor Lang and student Thomas Yuen.

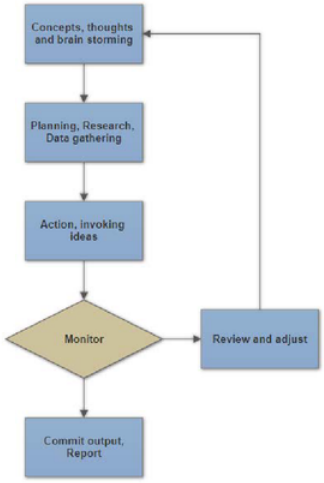

Figure 1 Overview Project management Flowchart

Due to the time constraints and scope of the project, aspects have been dropped. This was in consideration to ensure that a body of work can be delivered at a set date. See figure 52 for the projected plan. The development of this paper has had many follies and delays resulting premature development of Zinc FDM see figure 53. Optimistically the development of Zinc metal FDM has shown promise to be furtherly investigated.

Should Magzinc prove to be effective FDM commercial exploration will be perused. These may involve medical, industrial and electronic applications. A utopic goal would to see Magzinc FDM machines with medical standard sterilizing (radiative) capabilities operating at surgical sites. A patient would have an implant designed and printed within hours pre-operation.

1.2 Thermoplastics

There are a wide variety of thermoplastics available commercially for FDM 3D printing to name a few PLA being most common, ABS (also common), Nylon (less common) and PEEK, a high-quality engineering filament (specialized). Due to the ease of ability to obtain these materials (costs and location see table 1) and to investigate similar homogeneous material property trends PLA and ABS have been chosen to be tested. Peek and Nylon have been made exempt due to their price costs and time costs for this preliminary study.

Thermoplastic	**Price Per Kilo (AUD)**	Source
PLA (Australia)	30	[3]
ABS (Australia)	30	[4]
Nylon (Australia)	55	[5]
PEEK (Europe)	952.48	[6]

Table 1 Common Thermoplastics price list

1.3 Zinc Metal

The concept of printing metals opens a Pandora's box for endless applications to which been found difficult with the limitations of plastics. Metals have already been 3d printed through SLS, plasma arc (welding) and re-castable resin bonded filament. These methods are expensive comparative to FDM, so it is desired to develop direct metal FDM printing. To do so this paper will examine creating a zinc filament (manufacturing process) and a method for FDM.

2 Literature Review

2.1 Thermoplastics and Zinc Comparison

It is important to recognise thermoplastics and Metals are very different materials, and ultimately will behave differently in the FDM process. However, the understandings gathered from thermoplastics may aid with metal FDM. The principles on the microscopic level from an amorphous thermoplastic and a metal can be idealised similarly. It is important to recognise correlation does not mean cause but this paper can try and learn from gathered evidence.

For example, in an amorphous thermoplastic the polymers are tangled, during melting then drawing (mechanical work) the density of the polymers increases and the tangle strangles are straighten into a semi-crystalline structure [7].The same can be considered for metals and alloys, the amorphous domains when worked result in the crystalline structures inhibiting strain.

Muthy shows that there is an increase in glass transitional temperature with worked amorphous plastics and lowered when annealed. This would be similar for metals as more energy is needed to massage structures in their transitional phases. Lower energy glass transition temperatures are desirable, enabling better viscosity flow. During the manufacturing process of the filaments, heated rotary drive filament extrusion results working of the material. Suggesting for better prints to result from pre-annealing and post annealing.

Zinc has a very high melting point $(\sim 419.5℃)$ in comparison to PLA. Zinc also has high thermal conductivity $Solid\ (410.5℃) \sim 96 \frac{W}{mK}\ and\ liquid\ (419.5℃) \sim 164 \frac{W}{mK}$ [8]. This high melting point and high thermal conductive poses as many problems:

- May cause thermal creep up the filament into electronics specially the driving extruder motor. Motors usually have operating temperatures below $130℃$ [9].
- Premature cooling prior surface wetting. This may cause bad adhesion to cooled deposition material.
- High energy thermal demands for the hot end. The heat from the melting hot end may be pulled away from desired melting location.

Magnesium Zinc alloy dramatically lowers the melting point to $364\ ℃$, Mg 2% WP see figure 2. Beneficially providing better conditions for future Magzinc filament FDM. This alloy also causes a plastic/solid semi-liquid mushy zone. Thomas Yuen provided scanning electron microscope imagining of a zinc Magnesium (Mg 0.8 % WT) from thesis "*Novel zinc alloy castings for medical implants*" showing eutectic (mushy) amorphous/semi-crystalline zones and crystalline phase zones. This mushy eutectic phase will also aid in the deposition placement and structure as it will behave more viscous. Viscosity is important in FDM to prevent material running or spilling undesirably, a simple analogy is comparing maple syrup and honey on pancakes.

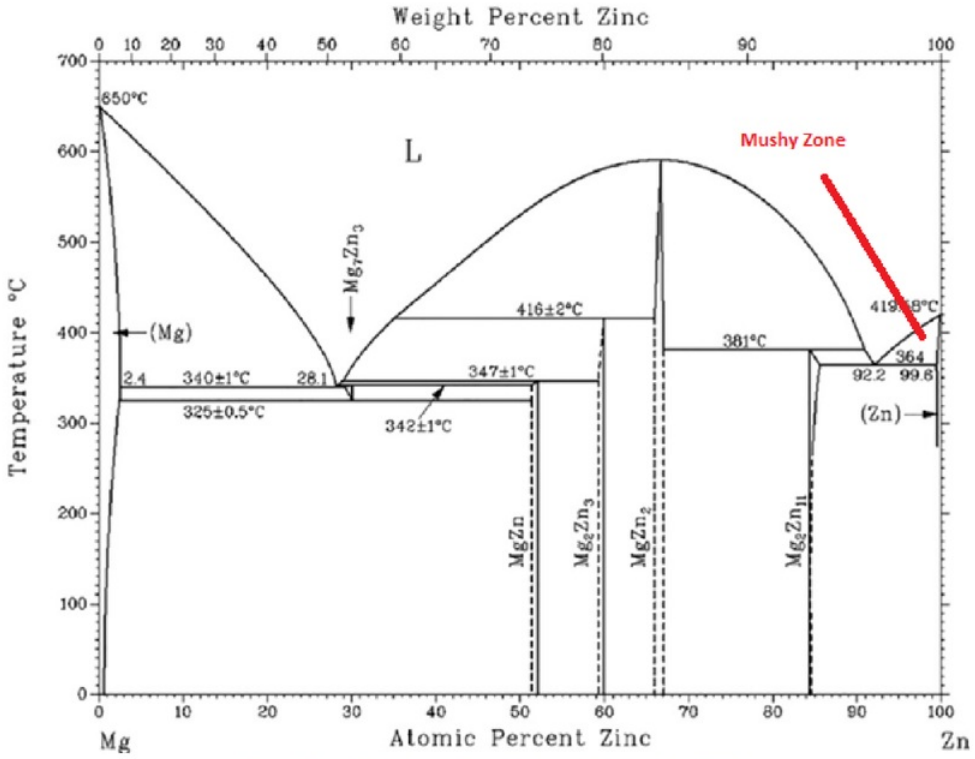

Figure 2 Zinc Magnesium Phase Diagram (C. Schneider, 2011)

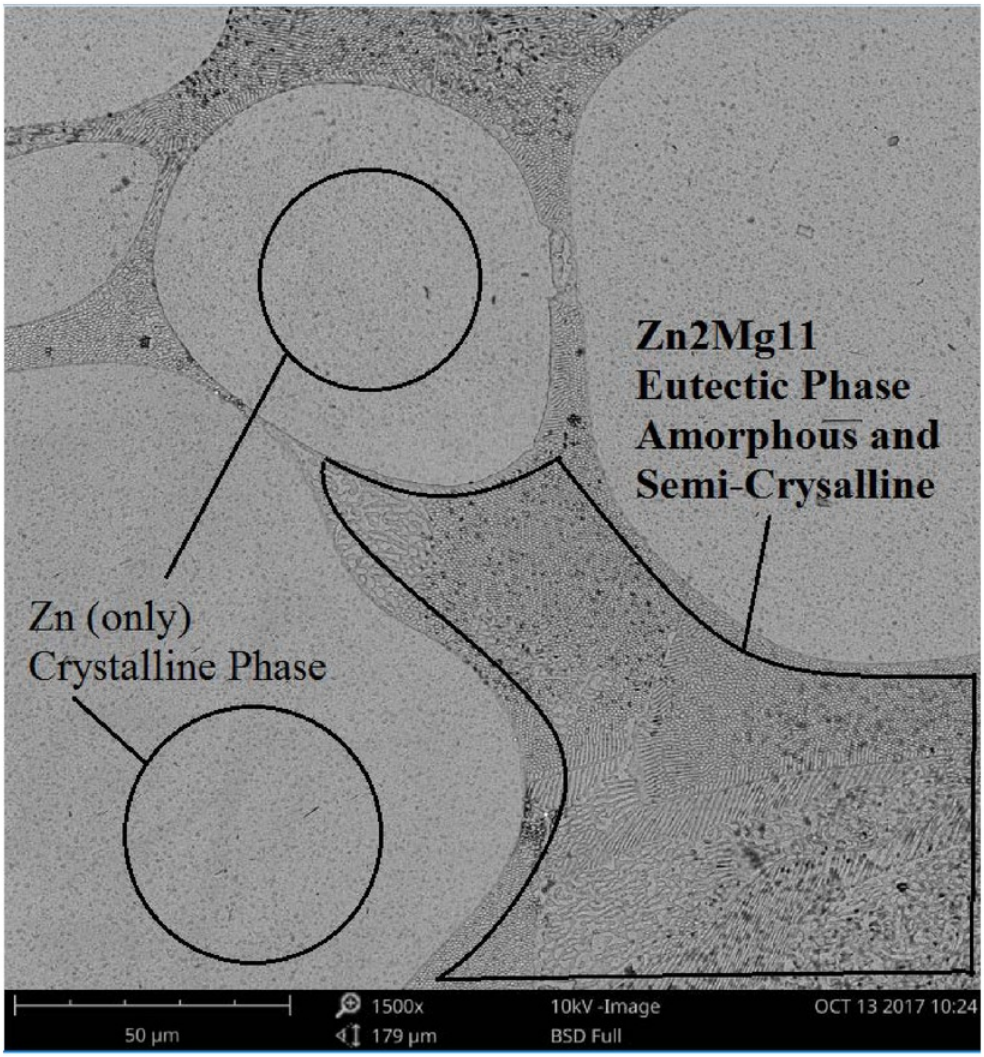

Figure 3 Zn- Mg 0.8%WT SEM scan Various phases

2.2 ABS and PLA

Current industry utilizes ABS and PLA FDM for rapid prototyping. PLA is used more readily than ABS due to ideal printing results (ABS tends to smell and warp). However final designs prefer to use ABS due to its greater durability. [10].

Ultimately the decision of thermoplastic type is determined by the end application of the artefact. These end applications have been proven to be vast, but with limitations of their structural, thermal and conductive capabilities.

2.2.1 Testing

Testing parameters are directly driven by the FDM print parameters. These are layer size, temperature rates, print head speed and (raster) orientation. This paper will highlight variations through first and second-hand research. Already there is vast amount of research concurred of plastic FDM from academic and non-academic sources. Second hand research will prove valuable due to time constraints of this paper.

This paper will attempt to consolidate as much primary information as possible which is limited by time and my understandings.

The following test conditions (see table 2) have been situated and will be attempted to be completed for PLA. Each condition will be tested from a base class settings, 200°C extruder temp, 60°C bed temp, 0.1mm layer Size, 80% infill and 60mm/s print speed, clear or white filament to be used to avoid pigment variation. The software utilized to generate machine code is Cura (version 2.7.0). Extruder setting will be calibrated to the machine to which is best to perform reliable filament beading.

Variable Category	Layer Size (mm)	Orientation (print head mapping)	Temperature	Print Speed	Chemical Bathing
Variable	0.3 (Drafting, rough) 0.1 (Fine)	5 orientations see figure	PLA 200°C $\pm$ 5°C ABS 230°C $\pm$ 5°C	Undetermined	Undetermined (project time).

Table 2 Variable FDM Plastic conditions

The specimen was designed from American Society for Testing and Materials (ASTM) specification for sub size T-bone specimens (see figure 4).

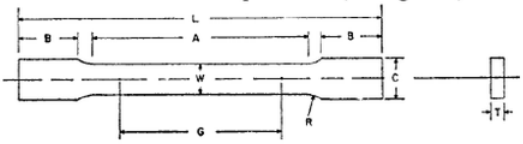

	Dimensions		
	Standard Specimens		Subsize Specimen
	Plate-Type, 40 mm [1.500 in.] Wide	Sheet-Type, 12.5 mm [0.500 in.] Wide	6 mm [0.250 in.] Wide
	mm [in.]	mm [in.]	mm [in.]
G—Gage length (Note 1 and Note 2)	200.0 ± 0.2 [8.00 ± 0.01]	50.0 ± 0.1 [2.000 ± 0.005]	25.0 ± 0.1 [1.000 ± 0.003]
W—Width (Note 3 and Note 4)	40.0 ± 2.0 [1.500 ± 0.125, -0.250]	12.5 ± 0.2 [0.500 ± 0.010]	6.0 ± 0.1 [0.250 ± 0.005]
T—Thickness (Note 5)		thickness of material	
R—Radius of fillet, min (Note 6)	25 [1]	12.5 [0.500]	6 [0.250]
L—Overall length, min (Note 2, Note 7, and Note 8)	450 [18]	200 [8]	100 [4]
A—Length of reduced section, min	225 [9]	57 [2.25]	32 [1.25]
B—Length of grip section, min (Note 9)	75 [3]	50 [2]	30 [1.25]
C—Width of grip section, approximate (Note 4 and Note 9)	50 [2]	20 [0.750]	10 [0.375]

Figure 4 ASTM Specimen deisgn [11]

From this the 6mm catogory was selected and design, see figure 5. The Computer Aided Design (CAD) drawings can be found at [12].

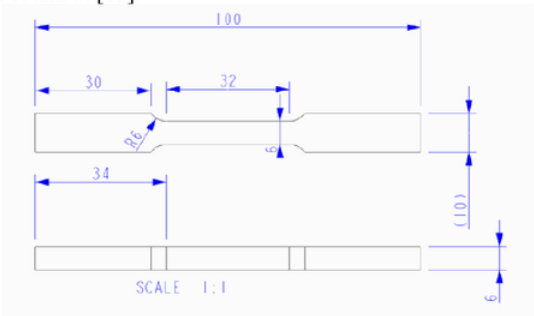

Figure 5 Creo CAD drawing

Layer size will range from a common draft (0.3mm) layer size to common fine or final (0.1mm) layer size for a part.

Orientation of T-bone specimens which has 5 possible tests see figure 6. this is decided by the way the print head extrudes plastic. These specimens are UP, A, 45A, 45,4545. Note when labeling the specimens great care is needed to understand. Orientations UP, 45A and A have the same XZ plane print direction see figure 7. Specimens 45, 4545 have the same print direction in XZ plane see figure 8. UP differs from specimen A due to the layer build direction. A's cross-section in the YZ plane, the filament travels transversely (see figure 9 into XZ or into or out of page) and it's layers going up in Y in the YZ plane. UP's cross section in the XZ plane has the filament see figure 7 and layers going up in Y direction. The specimens with 45 in the naming dictate a 45-degree rotation from A in both Z and X axis. The idea of orientations will show the difference of strength of layer adhesion and filament print direction.

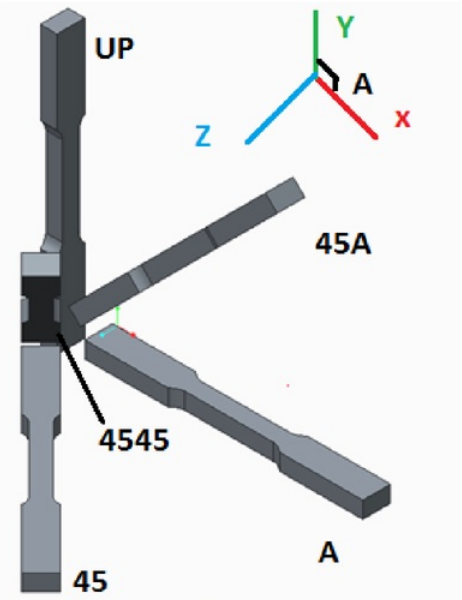

Figure 6 The five orientation Specimens in Cartesian coordinates.

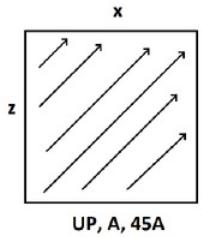

Figure 7 XZ plane filament direction single layer

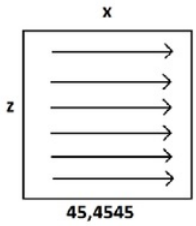

Figure 8 XZ plane filament direction single layer

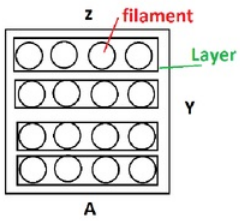

Figure 9 YZ layers and filament direction

2.2.1.1 Temperature of printing

Due to the nature of FDM **Temperature** manipulation arises residual stress in prints. The residual stress can be explored in post processing annealing of the plastic parts to increase their ductility. Temperature also results in the adhesive capabilities See figure 10 research by university of applied sciences and arts northwestern Switzerland, showing the collapse of deposition at mins and maxima temperatures (175°c and 275°c). figure 10 shows there is a goldilocks temperature (205°c to 220°c)

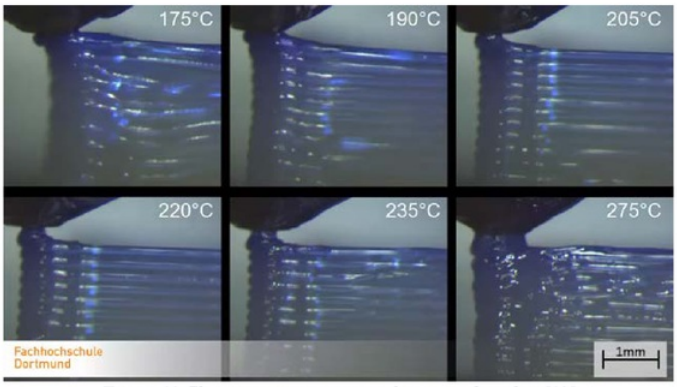

Figure 10 Changing temperature and structural quality [13]

2.2.1.2 Print head motion

Print speed dramatically effects the quality (structure) of print and ultimately changes the duration time for a print. Therefor structural comparability arises. This paper would like to discover more about this. However due to timing it may be omitted. The rate at which the printer head moves has a relationship with the flow rate, if not deposition structure is lost see figure 11 research by university of applied sciences and arts northwestern Switzerland.

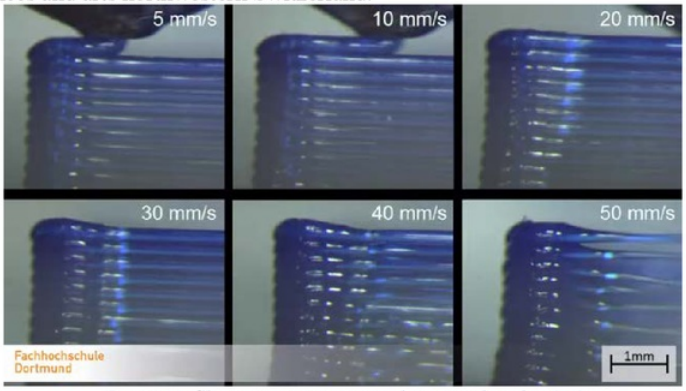

Figure 11 Changing temperature and structural quality [14]

Surface quality is a routine requirement for various manufacturing techniques such as high tolerance fitting, wearing and low friction operations. Pérez, demonstrates that the quality of the surfaces has a relational specification set by the printing head dimension parameters [15]. This is significant as Chang elaborates that surface finish is crucial to miniaturized samples for traditional manufactured components (rolled, subtractive manufacturing) [16]. This underpins a significant deviation to the mechanical properties in uniaxial tension regarding medical applications for 3d printing in conjunction with 3d scanning drives for high quality finishes and tolerances. [17].

It is for these reasons that the quality of surface finishing is essential when studying the structural properties of additively manufactured components. The motion of cheap 3d printers is dictated by open loop stepper motors driven by machine code (g-code usually). This motion results in a prints quality and ultimately mechanical properties. Normally at high speed and acceleration motion errors occur due to motion jerk and skipping from open motor system. M. Duan et al have developed a limited-preview filtered B-spline (LPFBS) method to reduce surface roughness see figure 12 and reduce time in prints [18].

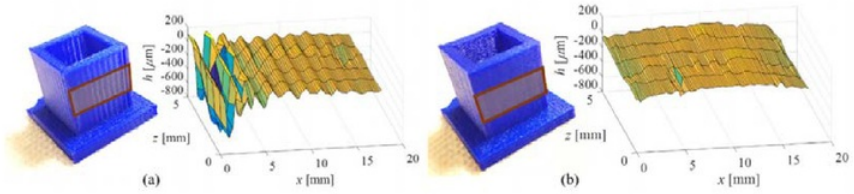

Figure 12 Non LPFBS method VS LPFBS method at 7 m/s2 acceleration limit [18]

Acc. limit	1 m/s^2	3 m/s^2	5 m/s^2	7 m/s^2	10 m/s^2
Printing time	3:59 h	2:42 h	2:22 h	2:12 h	2:06 h
Baseline					
FBS					

Figure 13 60mm/s flow rate, FBS reduce print time [18]

2.2.1.3 Post Processing

Chemical bathing has been utilized to improve the surface quality of PLA materials. [19] A solvent can be used to dissolve peaks and ridges on a print to then solidify gaps and valleys causing better layer adhesion and smoother surface finish see figure 14. This may be explored, see figure 15. This highlights the overall stresses have been reduced, better surface finish and tougher prints [19]. A bathing apparatus would be need. There are commercial bathing devices available however without stringent environmental control. In foresight, an ultrasonic transducer(s) were bought for acetone vaporization (no heating to avoid flash point for safety). This was proven successful to vaporize, but this has not been perused further do to timing and objective refocus for development of zinc FDM.

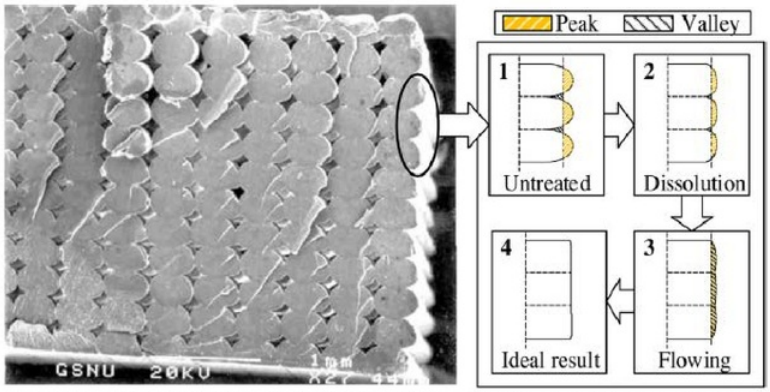

(a)Shape of deposited filaments (Ahn et al.,2002) (b)Process of chemical reaction

Figure 14 Process of dissolution and flow on the profile of PLA parts: (a) Shape of deposited filaments (Ahn et al., 2002) and (b) process of chemical reaction. [19]

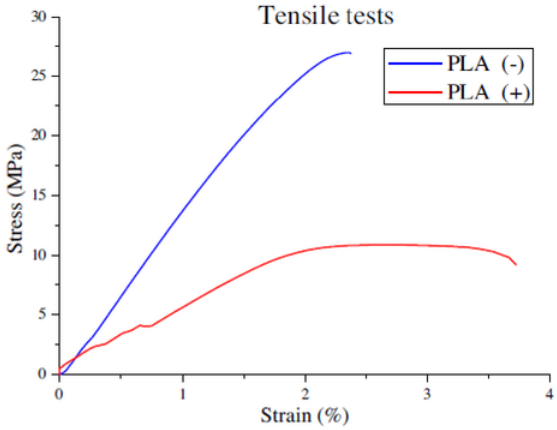

Figure 15 Comparison of the stress-strain curves before (−) and after (+) chemical finishing. [19]

2.3 Zinc Magnesium alloy

Zinc alloys have shown to retain use in biomedical applications. Dharam P et al detail Zinc alloys can be used as a biomedical implant which can be altered to be corrosive or non-corrosive with PLA coatings [2]. The Xi'an Aide Wansi Medical Science & Technology patent also shows promise of an "anti-corrosion high-toughness zinc alloy implant material capable of being absorbed by a human body." [20]. Zinc Alloys have great potential within the medical world, combining the FDM technologies would greatly aid design and use for biomedical implants.

Zinc alloy also being conductive allows for the use of FDM to make complex electronic trace circuity. Current methods of creating circuit board trace such as acid etching or Computer Numerical Control (CNC) machining great amounts of by product and time consumption. Zinc alloy circuit FDM also means rapid prototyping for electronic devices.

2.3.1 Zinc Alloy FDM printing method

There are no commercial available devices to FDM print zinc, therefore this paper will attempt to provide such method. The basic concepts of FDM will be retained from commercial opportunity such as CNC 3 axis control and filament extrusion. These opportunities will arise from combination of a Joseph Prusa i3 Mk2 printer and Dyze 500℃ hotend and extrusion system (see figure 16 and figure 17). They will be configured together and a printing chamber (see figure 19) made to provide a controlled inert environment. The Prusa i3 Mk2 printer utilizes a CAD model from open source thingiverse project [21].

Figure 16 Dyze hotend [22]

Figure 17 Dyze extruder [23]

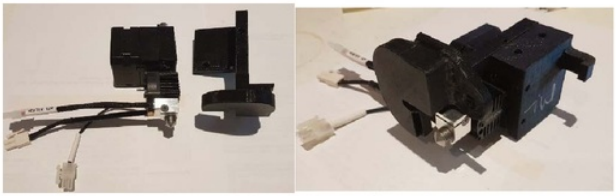

Figure 18 Printed Dyze adapter [24]

The chamber (see figure 19) has been designed to fit 60cm x 60 cm x 40 cm printers with holes to allow for Argon gas, filament and power cables. Argon gas was chosen to expel any moisture or reactive gases that could hinder Magzinc printing. An external chamber will be made to hold filament in similar inert conditions but also to store the filament. The chamber is made as a safety measure to prevent moister such as water to enter the nozzle which would could vaporize into pressurized steam. The chamber also prevents molten Zinc splashing outside the printer. The CAD and drawing files for the chamber can be found [25].

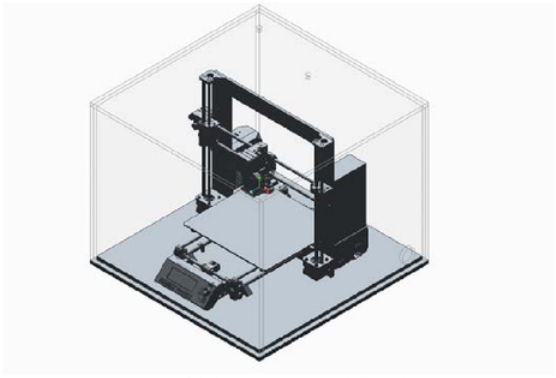

Figure 19 Prusa printer and Chamber

The chamber may need thermal captive properties to retain an environment in which residual stress of parts do not cause warping. This may be done by applying adhesive aluminum tape to the walls. Small holes positioned above the argon gas inlet to vent existing gases.

To find the argon fill rate the following equation. Assumptions were made such as no undesirable leakage and vacuum. The volume of the enclosure is 144 L, using a 55 to 65 CFH (25.96 to 30.68 LPM with ¾" to ½" orifice) [26] fills the chamber with argon gas in under 6 minutes. See equation 1.

$$\frac{v}{\dot{v}} = \frac{144L}{[25.96\,,30.68]\frac{L}{min}} = [5.54, 4.69]\,min$$

Equation 1 Chamber fill rates

Ultimately a vacuum would be preferable for the argon gas to enter, to prevent gas mixing. This would be to lengthy for this scope. To achieve a preferable environment the chamber should be filled at a laminar flow. This will prevent the mixing of gases and a smooth transitional level for the argon gas to fill.

2.3.2 MagZinc Filament

The zinc filament is not commercially available and will have be manufactured. There are various methods of manufacturing. Such as draw pulling, round milling and a propsal tangential lathe cutting. Drawing results in a closer tolerance (1.75mm) desired but is stage drawn. Therefore combination of two methods are usually done. The characteristics of zinc magnessium materials suggest it may have biomedical and electronic trace uses.

2.3.2.1 Round Milling and drawing.

This process of wire forming is used in Jewelry and industrial methods of making wire. Required machinery are a rolling mill and a die press (see figure 20 and figure 21). It involves milling a cast or turned cylindrical stock material, then pulling or pushing through a die cast. These methods are

scalable, and available commercially. A 14kg 2.3 mm spool of Zinc wire was purchased (sourced from Zinc galvanizing process) and processed by a local company to die pull to 1.76mm.

Figure 20 Rolling Mill [27]

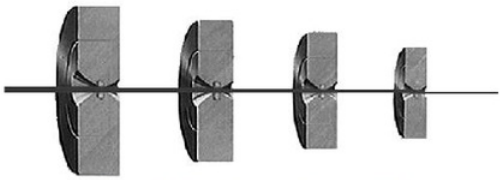

Figure 21 Wire Drawing Diagram [28]

2.3.2.2 Filament Extrusion machine.

Most Thermoplastic filaments are manufactured using heated extrusion. This uses a motor, to drive and heat pellets from the hopper via cork screw with the aid of heating elements. See figure 22 This method is effective as it can directly produce the correct diameter filament without post processing such as drawing.

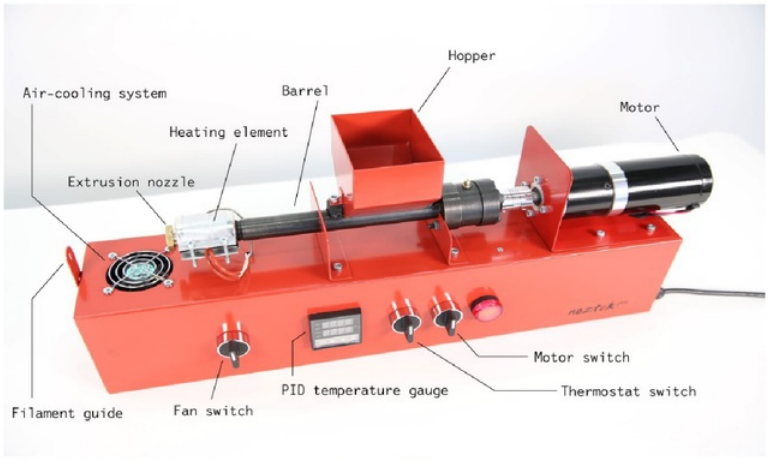

Figure 22 Heated Rotary Drive Filament Extruder [5]

Note, this method has been chosen to manufacture zing magnesium filament, a machine has been purchased however modifications will be needed to prevent oxidization and quality control. Modifications may prove to be like the modifications made to the printer.

2.3.2.3 Tangential lathe cutting

This paper proposes to create a wire from a stock by lathe tangential cutting. The theory is by utilizing off cuts of the lathe rotary machining process see figure 23. Limitations involve creating a tangential cutter, turning the stock material with enough angular momentum and ultimately Zinc machining characteristics.

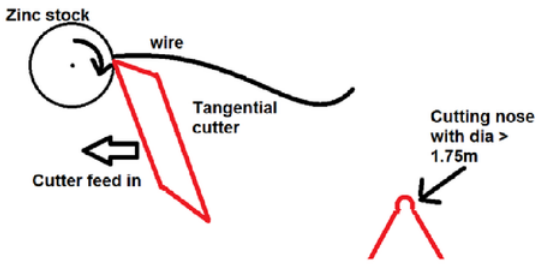

Figure 23 Tangential Cutting diagram

2.3.2.4 Storing and preparation of Zinc filament

As detailed Zinc should be stored in an inert environment due to possible containments. Formation of Zinc salts such as Zinc Chloride (hydroscopic) and Zinc Oxide can result in poor print extrusion. To reduce formation of salts, an argon chamber for the filament will be made accompanied with silicone gel satchels to absorb and remove moisture.

2.3.2.5 Adhession of filament.

Filament adhesion is an underpinning factor of the plausibility of FDM. A model for wetting theory developed by Thomas Young can be used to help predict PLA's adherence [29] detailing how a deposition of PLA has a completely wetting charactersitcs (wetting contact angle of 0 see Figure 25). See figure 24 showing the wetting charactersitic being more beneficial for surface bonding. The better surface bonding the more likelyhood of a successful print. Aiqiong et al state that the deposion slice thickness greatly attributes to the adhesive strength.

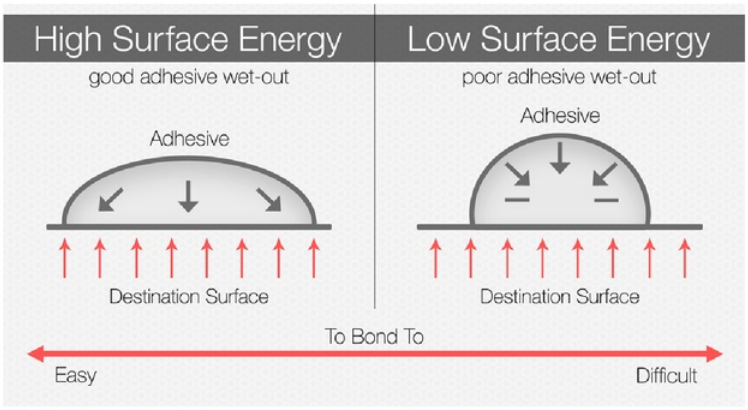

Figure 24 The adhesion process with high (left) and low (right) surface energy materials. [30]

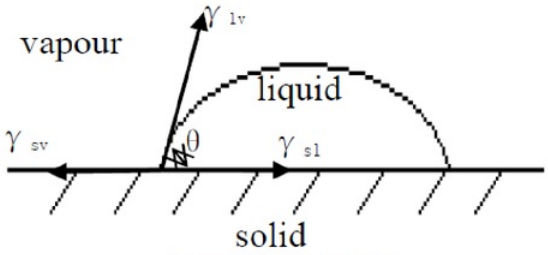

Figure 25 Wetting Angle [29]

3 Experimental Procedure

3.1 Thermoplastics (PLA)

The samples to be tested are printed using independent printing parameters as said in 2.2.1 Testing on an ANET A8, Cocoon Create and Omni3d printers (when available, iterations of parameters on a single machine to reduce variability errors). The g-code compiler will be Cura 2.7.

3.2 Tensile testing and Young's Modulus (PLA)

To examine the parameters they will be tensile tested with an MTS e42 tensile machine see figure 26 for method.

Step:	Description
1	Before powering machine ensure it is unobscured and safety is ensured. Wear protective goggles and any further protective wearables.
2	Power up a connected computer to the MTS e42 machine
3	Start the MTS machine, ensure that the emergency stop switch is extended out in the off position. (pull twist switch
4	Start the MTS software, and load a suitable profile (standard tensile testing profile). Edit to an ideal pulling rate and enter specimen dimensions.
5	Move the MTS jaws into placement (distance gauge of specimen between jaws.)
6	Clamp specimen into jaws by rotating locks equivalently to position specimen centered in jaws.
7	Verify safety and begin data login software and initiate tensile test (ensure system locks are okay, Interlock).
8	Save data by either export to text file or save project file. (Process though Spreadsheet)

Figure 26 MTS e42 Tensile test method

3.3 Printing Zinc filament

To print at higher temperatures a Prusa i3 MK2 was purchased along side a Dyze Extruder system (500°C). These were combined. Intial parameters of printing Zinc filament will require an inert environment, a high temperature hot end and suitable filament material. The inert environment is to elimite possible conaminations and unconrolled errors. A chamber to be filled with argon gas was developed. Attempts of the printing process will be alike the thermoplastic printing, with different temperatures (g-code from Cura 2.7). The print bed should be removed replaced with sheet metal (stainless steel) to withstand higher temperatures and anti-alloying properties. Metal FDM will be more wearing on the print nozzle initial testing will use a hardened stainless-steel head. This may be replaced with a more durable material like titanium or tungsten later. It is important to use stainless steel were possible interactions with liquid zinc to avoid unwanted alloy fusing (This was found problematic in results). A jet stream of Argon gas aimed at the nozzle may be suited help layer formation.

The project goal, to print zinc filament with these concepts were carried out in the feedback loop manner see figure 27.

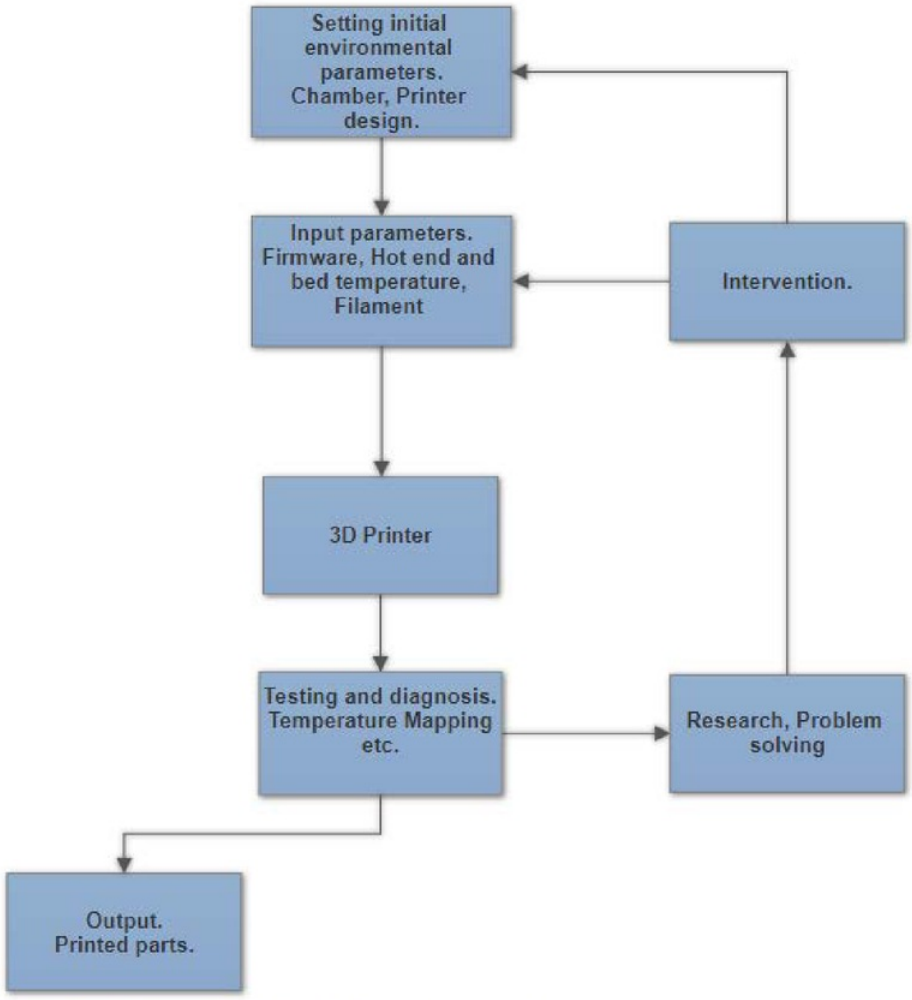

Figure 27 Zinc 3D printing project flowchart Thermoplastic and Metal FDM comparison

4 Results

4.1 Thermoplastics

When attempting to tensile test the specimens it was found difficult to align with in the jaws. A jig was made to help position specimen and placed on either side to secure in the MTS e42 Jaws (see figure 28, figure 29 and figure 30). The CAD drawings for the jig can be found, [31].

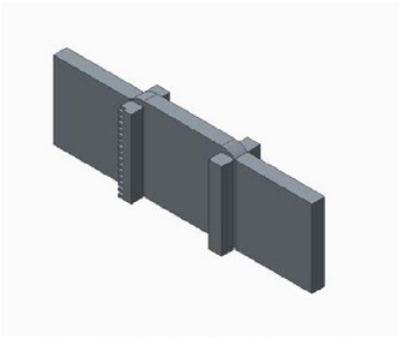

Figure 28 CAD drawing of placement jig

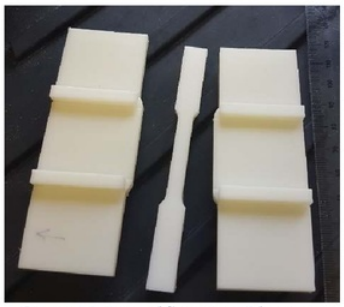

Figure 29 Jig and Specimen Placement

Figure 30 Jig and Jaw placement

4.1.1 PLA Tensile and Young's modulus

Specimens was loaded into the jaws with a jig, then tested with method detailed in figure 26.

4.1.1.1 PLA Orientation

The data recorded from the orientation can be found, [32]. Limitations in the test, there were notable error in testing the orientations. A common error which occurred were failures at the upper neck of the t-bone with different widths, in this instance we can assume the data does not test the desired thickness of the specimen. Critical failures were noticed to be along the printing layer plane see figure 31. The UP configuration was very weak and samples snapped in transport.

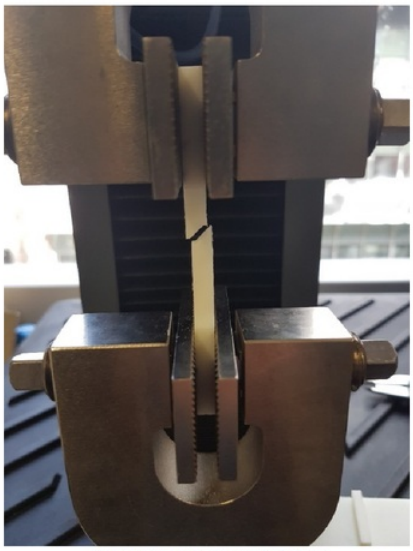

Figure 31 A45 Critical failure

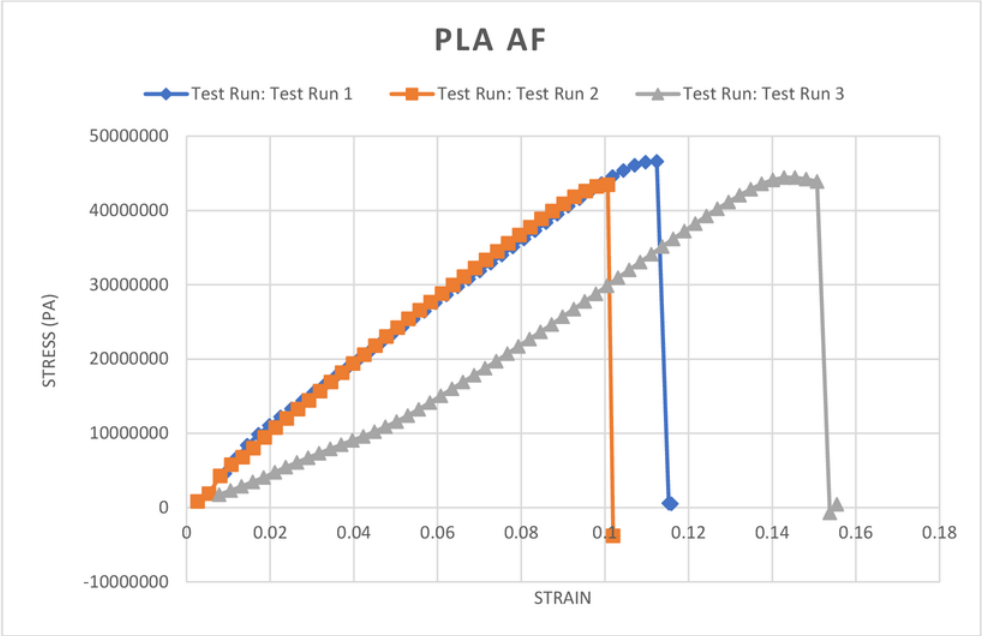

Figure 32 PLA AF Strain Stress curve

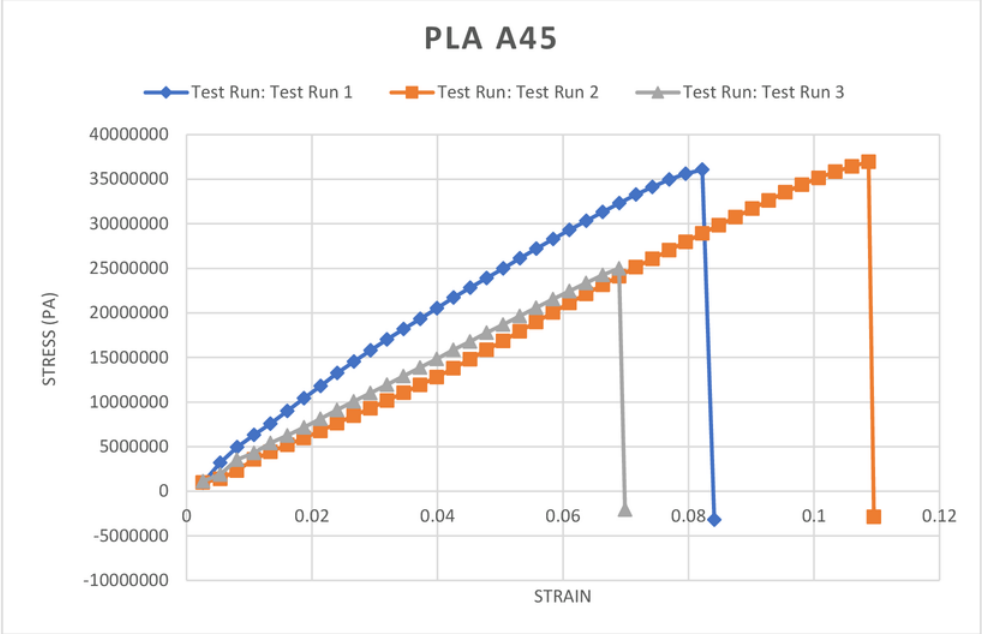

Figure 33 PLA A45 Strain Stress curve

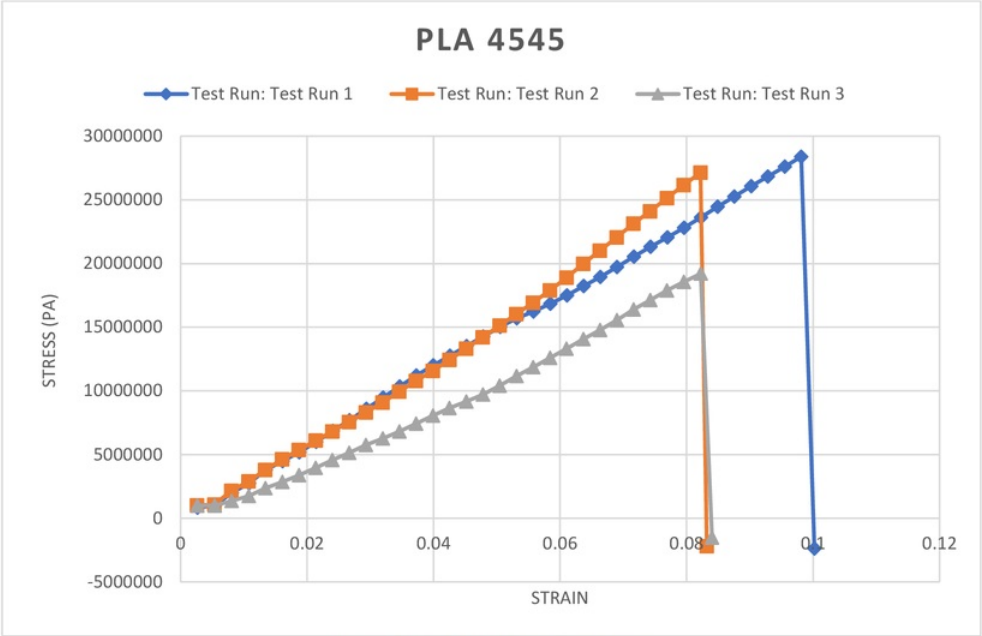

Figure 34 PLA 4545 Strain Stress curve

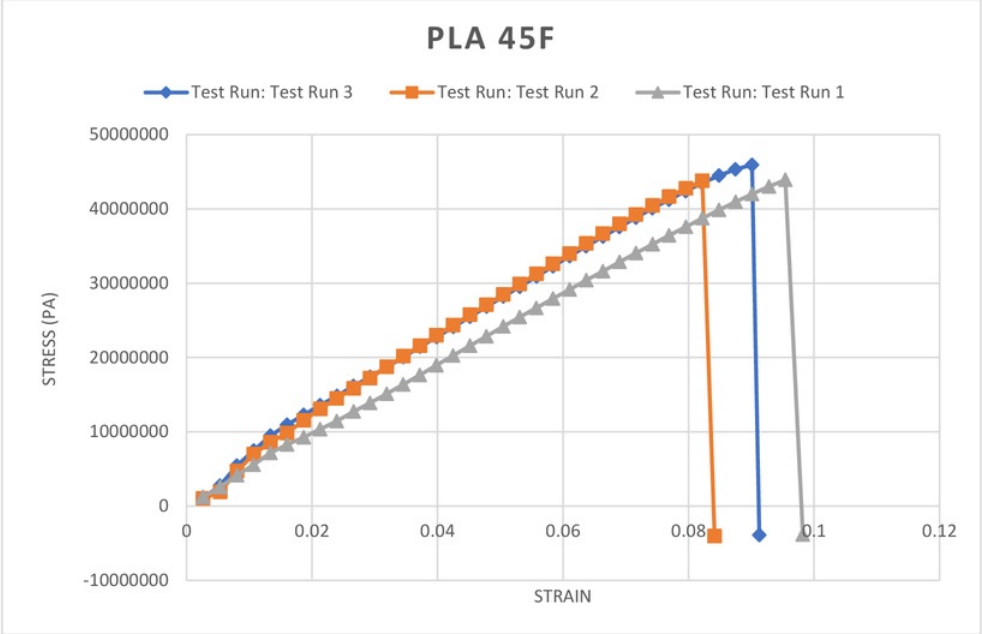

Figure 35 PLA 45F Strain Stress curve

4.1.2 ABS injection mold vs ABS FDM

The work compiled by Ahn et al (2002), explore the loss of strength for ABS between traditional Injection molding manufacturing and FDM. See figure 36. The raster angles dictate the filament deposition direction. This concludes with results gathered from PLA testing's.

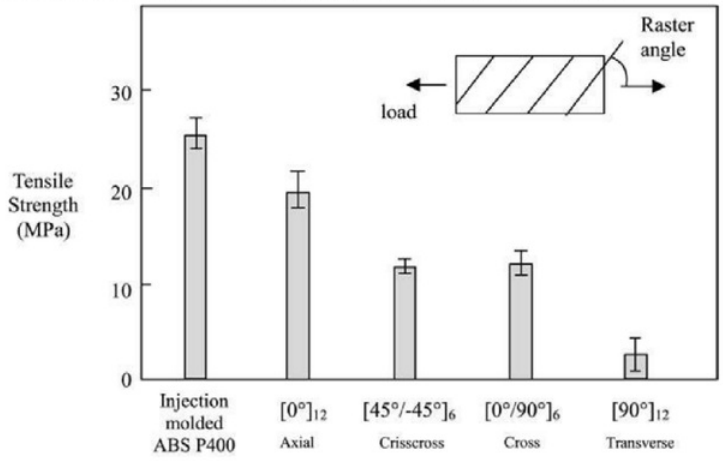

Figure 36 Table Tensile strength of injection mold vs FDM [33]

4.2 Zinc Fused Deposition Modeling

The focus of Zinc FDM proved to be challenging. The goal of printing a part in zinc was not achieved but progress was made. The printer was assembled in week 6, the Dyze system was installed. The printer was placed into chamber built (by METS Macquarie Univesity) and handles were installed to ease lid removal. The final system see figure 37 was assembled to begin testing late in week 8-10.

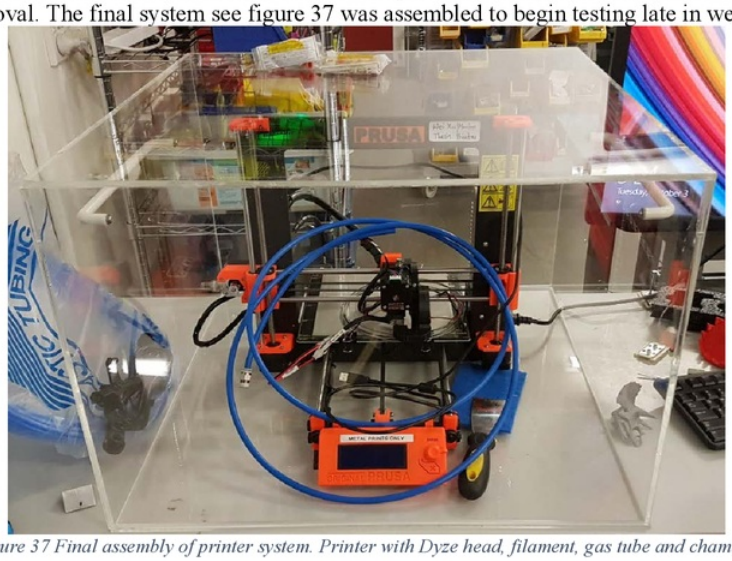

Figure 37 Final assembly of printer system. Printer with Dyze head, filament, gas tube and chamber.

The Dyze 500°C system which was stated easily compatible with Prusa i3 was false. The installation, running and optimization of the extruder proved to be very challenging and dramatically delaying the project. The delays to get the head to reach above 400°C was around 5 weeks. From week 7 over the

university break to week 12. The approach to solve this led to many iterations of figure 27. There were consults with the Dyze technicians operating in Canada (international delayed response time). To which unveiled no actual previous use of their high temp model, no firmware to update the printer. The following attempts were invoked:

- Firmware creation and flashing to increase temperature limits and read correct temperatures.
- Development of a parallel step-down thermistor resistor to increase the accuracy of thermistor.
- Inline Power regulator installation (buck boost converter or mosfet) between hot end and main board.
- Replacement of the mini Rambo 1.3a main board with Ramps 1.4.
- Replacement of the Dyze hot end (purchase of two Dyze system) prevent alloying of heat block.
- Heat mapping and thermal insulation containment to prevent heat loss.
- Removal of oxidization on filament to promote thermal transfer.

The progress resulted in a combination of said attempts. The status of the printer shows the ability to melt zinc see 4.2.8 Zinc Deposition output.. The printer has a new extruder head, added insulation, no power regulator and updated firmware.

4.2.1 Firmware and Temperature control

The Dyze system provides a tutorial to modify a marlin firmware. Marlin software is the machines operating systems to interoperate g-code and control machine. The available open source code was limited, the code being incomplete caused additional code to be made. Additional libraries and temperature tables needed to be added and modified. The code was compiled using Arduino 1.6.8 software (this is a must as newer and older version do not work) saving as a hex file. The hex file was then uploaded using the Joseph Prusa firmware updater figure 38. The Marlin firmware will be provided as a compressed folder as the software would be futile to include in this paper. Programs will be listed and download Uniform Resource Locators (URLs).

The following links are accessed and made live with date of paper. If URLs die contact author for possible access.

- Marlin-1.1.x Prusa i3 mk2 modified code, https://1drv.ms/f/s!Aki0NirSTu333AxEkahQdg1XUcvJ Accessed 6/11/2017.
- Arduino 1.6.8, https://www.arduino.cc/en/Main/OldSoftwareReleases#previous Accessed 6/11/2017.
- Prusa i3 MK2 driver downloads (version 1.9.0), https://www.prusa3d.com/drivers Accessed 6/11/2017.

The temperature table was modified using new data from the Dyze technician correspondence, however temperature values were still incorrect. These can be found in thermistortable_66.hh file.

Prontface, a program for controlling Marlin based printers was used to cycle temperatures and control motors.

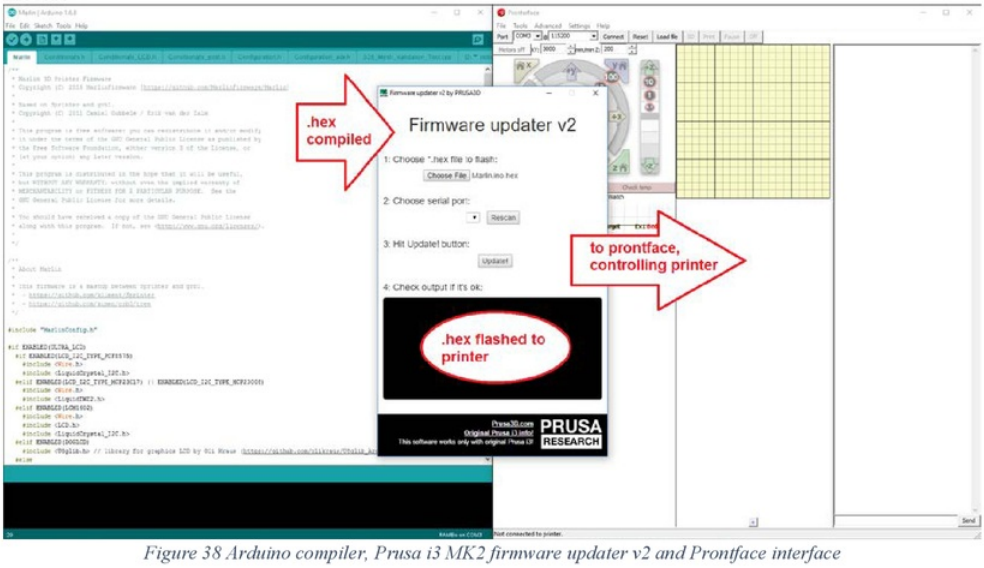

Figure 38 Arduino compiler, Prusa i3 MK2 firmware updater v2 and Prontface interface

4.2.2 Parallel Thermistor

The Rambo 1.3a board had errors reading the Dyze thermistor ($\sim 4.7M\Omega$ at room temp), a parallel thermistor-resistor was idealized to help with the boards temperature handling. A parallel thermistor was considered to lower the thermistors error rates and to make it make it more compatible with the Rambo 1.3a board. The board interprets a Negative Temperature Coefficient (NTC) thermistors value with an Analog digital conversion (ADC) circuit. The voltage of the circuit is an inverse linear relationship of ADC values from 0 to 1023. The higher the temperature the lower the ADC value. The value of the parallel resistor (R_2) was calculated to be $122.5k\Omega$ from the equivalent resistor at equivalent temperatures see figure 39.

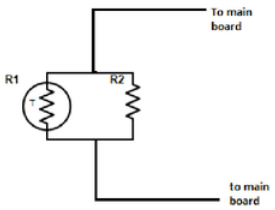

$$R_1 = thermistor\ resistor = 4.69M\Omega\ @\ 25\ ℃$$
$$R_2 = parallel\ resitor = 122.5k\Omega$$
$$\frac{1}{R_e} = equivelent\ resistor = \frac{1}{R_1} + \frac{1}{R_2}$$

Figure 39 Parallel Thermistor

This was confirmed with Dyze technician, showing that the ADC resolution is also increased with the parallel system see figure 40. This was abandoned as a new temperature table would have to be made for new ADC values. (project time restraints).

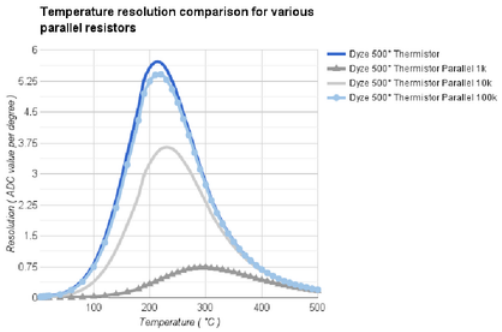

Figure 40 Dyze ADC resolution for parallel resistor.

4.2.3 Hot end power management

An issue was suspected raised from increasing the power consumption of the hot end. The system was not made for high end temperature hot end resistance heaters. There were two methods developed (buck booster and mosfet power recircuit), only the buck boosted tested.

4.2.3.1 Buck booster (step up)

A buck booster [34] was placed in line with the heater, to help buffer the mainboards power consumption. The buck booster system utilizes a switching capacitance and induction to step up the power provided to the heater. This did not work as the induction coils overheated due to the already switching signal from the main board.

4.2.3.2 Mosfet Power redirect

This method of utilizing a mosfet switch to use the main board heater signal to use a secondary power source. The mosfet and power source was sourced but not tested due to timing (shipping transit from

china delayed). The power source was a 12v 30amp power brick (15 more amps then the main board) which arrived dead on arrival.

4.2.4 Board replacement

A new board (Ramps 1.4) board was purchased to replace the Rambo mini 1.3a due to concerns failure to flash the firmware. Fortunately, the board was flashed and reconstruction was not needed.

4.2.5 Dyze hot end replacement

The Dyze hot end heater block had to be replaced due to it being made from aluminium. This cause unwanted alloy structure destruction when zinc filament contacted with the heat block see figure 41.

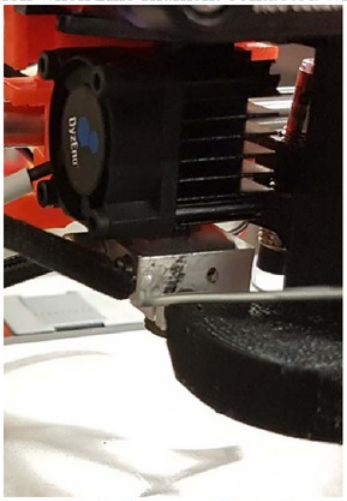

Figure 41 Aluminium Alloy erosion.

4.2.6 Heat Mapping and thermal insulation

The major issue for this project was achieving the right temperatures. The temperatures were attempted to be read with a K thermal couple and thermal IR laser sensor (thermal gun). Then to use these measurements to calibrate the printed temperature tables. These methods were primitive and limited to thermal contact with the probe (also loss of heat creep along the wire) and the emissivity limits and location accuracy of the thermal gun. Note two thermal guns were use one RS components and one NDi gun. This resulted in the purchase of a FLIR ONE Pro android thermal imaging camera (-20 → +400 °C, with ±2°C ,160 x 120pixel) see figure 42 [35]. Note testings were taken in (lab) room temperature environments.

Figure 42 FLIR ONE Pro android camera [35]

This camera help imensly with the ability to temperature map the system. Intially the system showed great amounts of thermal creep into the extruder motor and along the heater and sensor wires see figure 43.

Figure 43 Initial thermal imaging of Dyze extruder system. Motor block 59.1°C nozzle 150.9°C

This lead to the pursuit of thermally insulating the heat block. Solutions such as Boron Nitride paste, Ceramic wool wrapping and aluminum foil wrapping. These were all dropped and a ceramic (volcanic ash 600°C *max*) woven cloth wrapped and held in place with kepton tape (260°C max). This required

stringent safety precautions see figure 44. The fabric was wetted with alcohol to prevent airborne fibers.

Figure 44 goggles, mask, gloves, ceramic cloth, kepton tape and alcohol wetting.

The thermal insulation was installed and then reimaged see figure 45. The insulation wrapped the hot end heat block with insertions for the nozzle and filament entry tube.

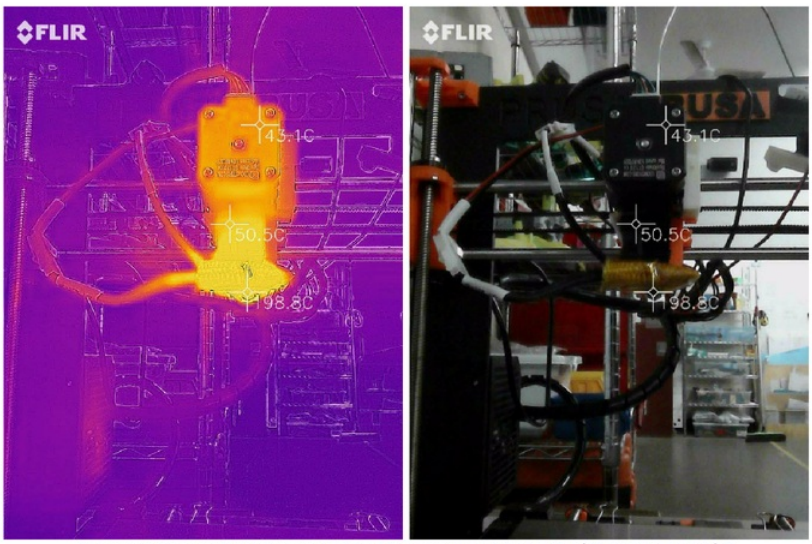

Figure 45 Thermal insulation modified Dyze system. Motor 43.1°C, Nozzle 198.8°C

4.2.7 Zinc filament

Zinc wire sourced From Metal Sprays Supplies Australia, a 14kg spool was purchased [36]. The spool, 4 mm zinc 99.99% drawn down to 1.78 mm. The quality was suitable, even though being drawn and worked the zinc filament was malleable, ductile and soft. There was a light formation of dull surface oxidization. This was then polished with sand paper (600 grit) then scotch bright (to prevent waste to enter the extruder head), trimmed to a spear point for ease of insertion. Note the gear teeth of the extruder drive can be seen see figure 46.

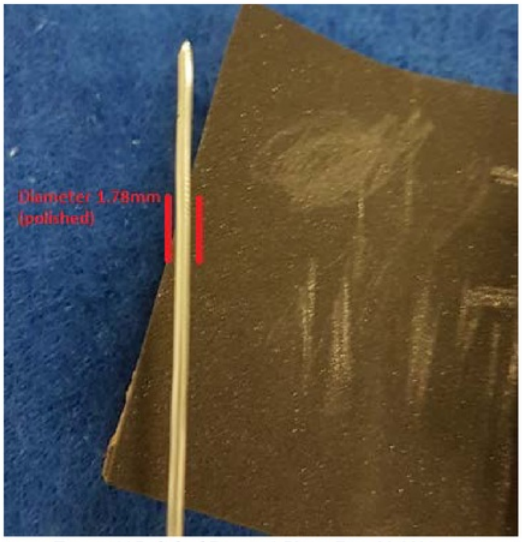

Figure 46 Polished Drawn 1.78mm Zinc 99.99% wire

4.2.8 Zinc Deposition output.

The results of the thermal insulation and firmware update allowed the printer to reach 418°C see figure 47, this was a crucial. The hot end began to exhibit a droplet of zinc see figure 48. This moment backed by the 12 weeks work was achieved when Doctor Wei Xu walked into the lab to review (impeccable timing Doctor Wei Xu!).

Figure 47 thermal insulation Set 420°C, nozzel 418.0°C

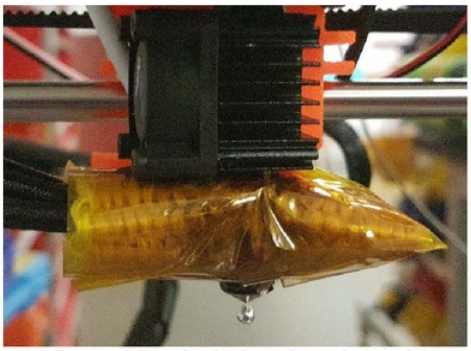

Figure 48 Zinc droplet formed at end of nozzle

The droplet formed, then dropped onto the stainless-steel bed below. This made a flattened puddle. Replication was then attempted, two droplets formed, one (the largest) was then removed with tweezers the other was then left to cool on the nozzle (heater and machine off). The droplet that formed the puddle was removed and split in two to view the structure see figure 49. The structure was crystalline characteristic.

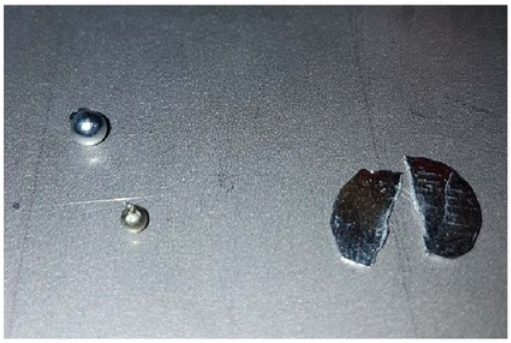

Figure 49 Top left tweezered droplet, below cooled droplet and far left puddle droplet split

5 Discussion

From the information collected Zinc FDM shows plausibility. Utilizing current thermoplastic FDM and Zinc Magnesium technologies has and will continue to aid in the development of Metal FDM.

The project was rife with errors. Error some which were human based and some from approximations.

5.1 Thermoplastics

5.1.1 PLA FDM

Reviewing the data collected (see figure 32, figure 33, figure 34, figure 35), 45F orientation seems to be the strongest with the highest UTS, AF having the better ductility and when rotating the orientation print around the Z and X axis (making the part proud from the bed) the weaker, the less ductile and fragile the part become (resemblance in the UP parts breaking in transport).

It was noticed that the primary UTS (45.9 MPa for 45F) was near to secondary source reported UTS, the Young's' modulus (0.51 GPa for 45F) was off by a factor of 10 (UTS 37 MPa, Young's modulus 4 GPa [37]). Explanations for this is, the cross-sectional area is of 80% to solid PLA, the PLA filament was not pure, the lamination adherence strongly dictates minimums for the prints ductileness and strength. Meaning 3d printing unless overcoming this factor (possibly through chemical bathing) it is weaker than traditional methods of manufacture. This was also exemplified in [33] which showed a 70% reduction in UTS.

There was a limit to the accuracy of the tensile machine, some came from the human error of incorrect placement of specimens. In occasion one of the proud from bed tensile piece snapped in two while clamping the tensile machines jaws. This error was the reason for the design of a jig. The jaw design also had no indication of tightening which caused offset in the two-ended clamping. This no doubt would cause torsional stress on the parts which would have most likely affected the results.

A limit was to the machining ability of the printer itself. Open motor FDM is subjected to jerking, placement skipping and oscillations (vibrations). This would have also impaired and skewed tensile results. Averages were taken of samples in attempt to mitigate this error. Another limit was the tensile strain gauging, a more accurate device such as an octo-extensometer would mitigate this error.

5.2 Zinc FDM

During the preparation of melting zinc, there were various proposals to address issues found heating the extruder. The compatibility of current high temperature extruder commercial products (Dyze) are not suitable for Zinc FDM. It would be advisable to develop a Bowden extruder system that removes the motor from the extruder head with ceramic insulation to prevent heat creep and heat loss. This is due to the nature of high temperature operation and heat loss. The heat mapping proved valuable information in designing thermal insulation. There was a great reduction in heat transfer from the nozzle to the motor block with the install of the woven ceramic insulation.

Another feature not previously shown, the second Dyze system was tested with PLA filament, which exhibited poor printing qualities due to the interference of the blunt nozzle head. The blunt nozzle head heated would cause re-melt of deposition material, a sharp nozzle would be beneficial.

In theory the parallel resistor system will increase the resolution ADC temperature handling.

Cleaning and polishing the Zinc filament will aid in the transfer of heat from the extruder but also prevent nozzle clogs.

A simple observation of the zinc droplets. The zinc has low viscosity and has an ideal surface energies and tension. The oxidization is low for rapid cooling but over time colour distortion occurs. The oxidization would prevent the adhesion. This oxidization stresses the importance for an inert environment. Rapid cooling of the deposition material would also prevent this oxidation but also aid in the deposition placement (essentially freezing material in place). An argon jet stream that is temperature controlled would be suitable.

Due to zincs, low viscosity it would suggest having print movement jerk low to assist in deposition placement. This factor may not be exhibited in a mushier eutectic phase Magzinc filament.

The Zinc droplet when landing on the stainless-steel surface made wet droplet characteristics. In consideration of Aiqiong et al's work this insinuates for PLA good adhesion qualities.

For the success for Zinc FDM, the ability to produce zinc tracing for electronics exists. Printing on thin glass or fiber glass sheeting (most likely) to be removed could provide a novel way of manufacturing low quantity highly complex circuitry.

6 Conclusion

There is a correlation for thermoplastic 3D printing process and final deposition material. Printing parameters alters the final qualities of deposed material and the print. This will be taken into consideration in developing Zinc 3D FDM printing. The precautions and gathered understandings shows promise and will help for a successful Magzinc FDM development. Zinc magnesium alloys exhibit vivo biocompatible characteristics which extends the pursuit of Magzinc FDM. The future works will no doubt be challenging but also rewarding.

7 Future works

The nature of this study was incomplete, due to time constraints. The results found showed promise of metal FDM success, so there will most likely be further development of zinc FDM. In correspondence with Dr Wei Xu, a biomedical Magzinc 3d printer may be pursued commercially. As mentioned it would be ideal to make a printer from scratch to have ultimate control of the machine. A specialized Bowden extrusion system see figure 50 and figure 51 would have to developed.

Future possible metal Magzinc FDM printer, optimistically would have:

- An enclosing chamber that aided to structural integrity.
- Vibrational dampening.
- Closed loop servo motion control.
- Inert temperature environment control.
- Remotely driven Bowden extruder system.
- Ceramic isolated heating blocks with liquid cooling. To prevent heat creep/loss.
- Wireless heat mapping monitoring system (similar to raspberry pi webcam monitoring). Beneficial for stress mapping and characterization.
- Sterilizing capabilities to medical and surgical standard for immediate vivo implants.
- Filament run out or snagging sensors to prevent failed prints.
- Power fail safe for power termination, a power cut interval to save a print progress for recovery.
- A streaming jet of argon at printer nozzle for temperature control.
- A Sealed band nozzle heater and high heat capacity metal heat block for uniform filament heating.
- Titanium nozzle to resist wear and alloying.
- Possibly a secondary high temperature plastic extruder for support creation. The plastic would have to be designed suitable for zinc FDM and post processing.

Future work will require significant funding, currently there has been interest in the project. Indirectly from Government from CSIRO and Chinese investors. The funding off-cuff estimate for a prototype would exceed $50,000 AUD.

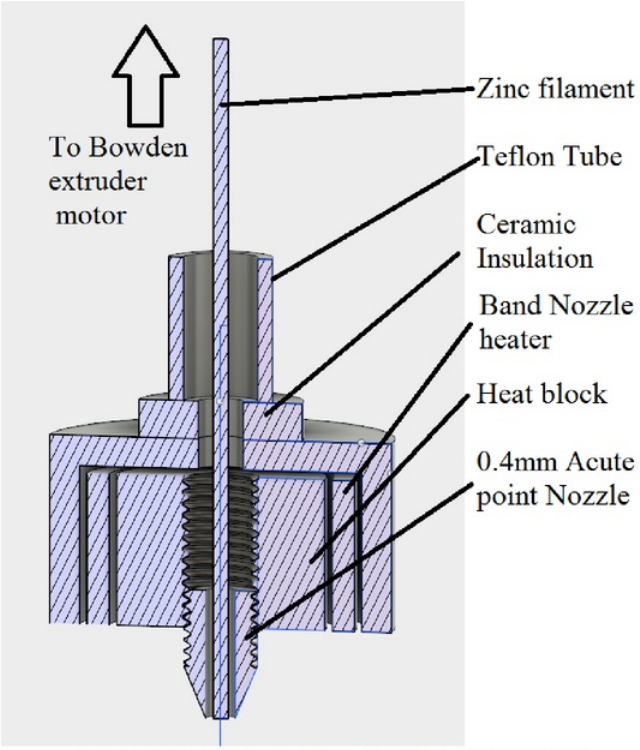

Figure 50 Cross-sectional mock up High Temp of nozzle redesign

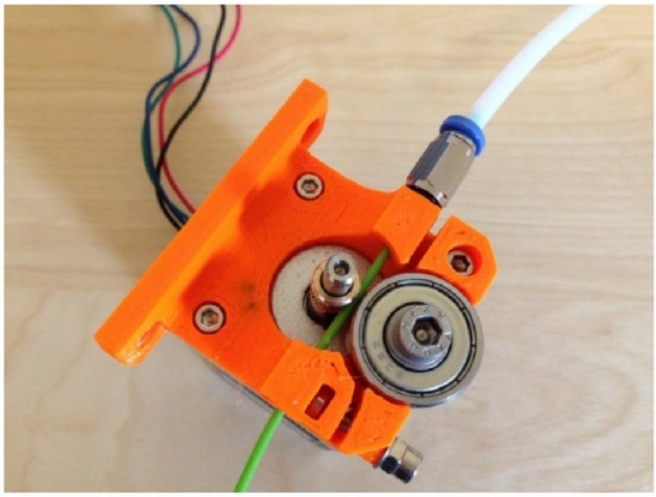

Figure 51 A conventional Bowden extruder motor design, with teflon tube [38]

8 Appendices

8.1 nomenclature

Abbreviation	Meaning
FDM	Fused Deposition Modeling
SLS	Stereolithography
ABS	Acrylonitrile-Butadiene-Styrene
PLA	Polylactic acid
MagZinc	Zinc Magnesium alloy 0~5%
CNC	Computer Numerical Control
CAD	Computer Aided Design
URL	Uniform Resource Locator

8.2 Planning

The project ended up deviating due to bureaucracy, ordering parts and delivery timings.

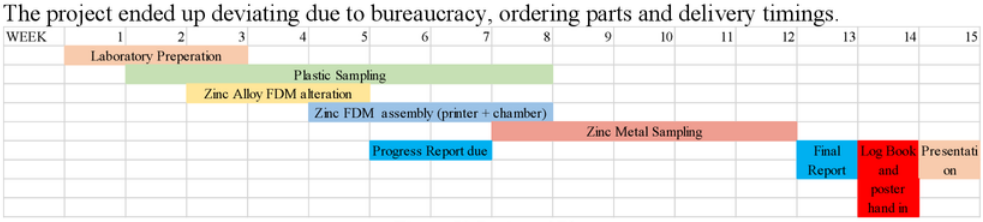

Figure 52 Projected Plan

This plan has been adapted from the deferred plan. If the project were to pinpoint its beginnings was at the Zinc alloy FDM alteration in week 3.

Figure 53 Actual Plan

Consultation Meetings Attendance Form

Week	Date	Comments (if applicable)	Student's Signature	Supervisor's Signature
	20/2/17	Initial Questions, -Standards -Associates	Marlon Leong	
	9/3/17	Filament Purchase	Marlon Leong	
	1/3/17	Wei Xu Settings For Metal Printer	Marlon Leong	
	6/3/17	Meet with Super Weekly lab meeting	Marlon Leong	
	24/08/2017	Wei Xu meeting	Marlon Leong	
	28/08/17	Wei Xu Filament. chamber. Argon gas, Commercial	Marlon Leong	
	7/09/17	Wei Xu Meeting	Marlon Leong	
	12/09/17	Wei Xu Range 14	Marlon Leong	
	3/10/17	Wei Xu meeting about [illegible]	Marlon Leong	
	16/10/17	Film Camera	Marlon Leong	

9 Bibliography

[1] K. Brans, "3D Printing, a Maturing Technology," *IFAC Proceedings Volumes,* p. 468–472, May 2013.

[2] A. M. Dharam Persaud-Sharma, "Biodegradable Magnesium Alloys: A Review of Material Development and Applications," *HHS Author Manuscripts,* pp. 25-39, 2012.

[3] X3D Australia, [Online]. Available: https://www.x3d.com.au/store/product/60036-filaform-pla-white. [Accessed 31 10 2017].

[4] X3D Australia, [Online]. Available: https://www.x3d.com.au/store/product/60117-filaform-abs-white. [Accessed 31 10 2017].

[5] X3D Australia, [Online]. Available: https://www.x3d.com.au/store/product/29276-x3d-pro-nylon-1-75mm-b-1kg-b-. [Accessed 31 10 2017].

[6] 3d4makers, [Online]. Available: https://www.3d4makers.com/products/peek-filament?variant=13704093060. [Accessed 31 10 2017].

[7] N. Murthy, "Glass Transition Temperature and the Nature of the Amorphous Phase in Semicrystalline Polymers: Effects of Drawing, Annealing and Hydration in Polyamide 6," *International Journal of Polymeric Materials,* vol. 50, no. 4, p. 429–444., 2001.

[8] American Galvanizers Association, "Zinc Metal Properties," [Online]. Available: https://www.galvanizeit.org/design-and-fabrication/design-considerations/zinc-metal-properties. [Accessed 31 10 2017].

[9] JVL Industri Elektronik, "Temperature for stepper motors," [Online]. Available: http://www.jvl.dk/1048/temperature-stepper-motor. [Accessed 31 10 2017].

[10] B. Hesse, "ABS OR PLA: WHICH 3D PRINTING FILAMENT SHOULD YOU USE?," 26 September 2015. [Online]. Available: https://www.digitaltrends.com/cool-tech/abs-vs-pla-3d-printing-materials-comparison/.

[11] A. S. f. T. a. Materials, "Standard Test Methods for Tension Testing of Metallic Materials," 2009. [Online].

[12] M. Leong, "Creo T-bone CAD," [Online]. Available: https://1drv.ms/u/s!Aki0NirSTu331hlxxxkjRoeURuEg. [Accessed 6 11 2017].

[13] Labor für Additive Fertigung, "FDM video analysis: Extruder temperature," [Online]. Available: https://www.youtube.com/watch?v=O70fJMMBmAI. [Accessed 31 10 2017].

[14] Labor für Additive Fertigung, "FDM video analysis: Printing speed," [Online]. Available: https://www.youtube.com/watch?v=BBQTD9_34sQ. [Accessed 31 10 2017].

[15] C. J. L. Pérez, "Analysis of the surface roughness and dimensional accuracy capability of fused deposition modelling processes," *International Journal of Production Research,* vol. 40, no. 12, pp. 2865-2881, 2002.

[16] Y.-C. J. a. Y. S. K. Chang Hee Suh1, "Effects of thickness and surface roughness on mechanical properties of aluminum sheets," *Journal of Mechanical Science and Technology,* vol. 24, no. 10, pp. 2091-2098, October 2010.

[17] H. N. C. a. B. M. Wu, "Recent advances in 3D printing of biomaterials," *Journal of Biological Engineering,* 2015.

[18] D. Y. C. O. Molong Duan, "A limited-preview filtered B-spline approach to tracking control – With application to vibration induced error compensation of a 3D printer," *Mechatronics,* pp. 1-10, 2017.

[19] Y. W. B. Z. Z. L. Yifan Jina, "Modeling of the chemical finishing process for polylactic acid parts infused deposition modeling and investigation of its tensile properties," *Journal of Materials Processing Technology,* 2016.

[20] X. A. W. M. S. &. Technology.China Patent CN103736152 (A) , 2013.

[21] DyzeDesign, [Online]. Available: https://www.thingiverse.com/thing:2239895. [Accessed 6 11 2017].

[22] "Hotend," [Online]. Available: https://dyzedesign.com/shop/hotends/dyzend-x-hotend/.

[23] "extruder," [Online]. Available: https://dyzedesign.com/shop/liquidcooling/dyzextruder-gt-coldend-extruder-1-75mm-liquid-cooled/.

[24] D. Design, "Prusa i3 MK2 with Dyze Design DyzeXtruder GT and DyzEnd-X," 10 April 2017. [Online]. Available: https://www.thingiverse.com/thing:2239895.

[25] M. Leong, "Creo Chamber Design," [Online]. Available: https://1drv.ms/u/s!Aki0NirSTu332R6zx7O0Ca_K15Q6. [Accessed 6 11 2017].

[26] WA Technology, [Online]. Available: http://www.netwelding.com/MIG_Flow%20Rate-Chart.htm. [Accessed 31 10 2017].

[27] [Online]. Available: http://www.ebay.com/itm/COMBINATION-ROLLING-MILL-80-mm-With-7-ROLLERS-ROLLS-SHEET-METAL-JEWELRY-TOOL-/152317893847.

[28] kingway technology. [Online]. Available: http://www.kingwaytechnology.com/elongation-of-wire-drawing-2/.

[29] Z. H. R. G. J. L. Aiqiong Pan, "Effect of FDM Process on Adhesive Strength of Polylactic Acid(PLA)," *Key Engineering Materials,* vol. 667, pp. 181-186, 2015.

[30] E. Pearlman, "Surface Energy and Labels: The Unscientific Guide," [Online]. Available: https://www.onlinelabels.com/Articles/label-surface-energy-guide.htm. [Accessed 31 10 2017].

[31] M. Leong, "Creo T-bone jig CAD," [Online]. Available: https://1drv.ms/u/s!Aki0NirSTu332SDZYF3WyxjgcPv-. [Accessed 6 11 2017].

[32] M. Leong, "Excel sheet PLA oreientation tensile tests.," [Online]. Available: https://1drv.ms/f/s!Aki0NirSTu331xICNsm50RpBNLBn. [Accessed 6 11 2017].

[33] S.-H. M. M. O. D. R. S. W. P. Ahn, " Anisotropicmaterial properties of fused deposition modeling ABS," *Rapid Prototyping Journal,* vol. 8, p. 248–257, 2002.

[34] kc_circuits, "Boost Buck DC-DC Adjustable Step Up Down Converter XL6009 Power Supply Module," [Online]. Available: http://www.ebay.com.au/itm/Boost-Buck-DC-DC-Adjustable-Step-Up-Down-Converter-XL6009-Power-Supply-Module/222366949621?ssPageName=STRK%3AMEBIDX%3AIT&_trksid=p2060353.m2749.l2649. [Accessed 31 10 2017].

[35] RS Components Pty Ltd, "FLIR ONE Pro Android Thermal Imaging Camera, Temp Range: -20 → +400 °C, -4 → +752 °F 160 x 120pixel," [Online]. Available: http://au.rs-online.com/web/p/thermal-imaging-cameras/1368285/. [Accessed 31 10 2017].

[36] MSSA, "MSSA Arc Spray Wires," [Online]. Available: http://www.metalspraysupplies.com/wp-content/uploads/2016/01/MSSAARCSPRAYWIRES.pdf. [Accessed 31 10 2017].

[37] K. Giang, "PLA vs. ABS: What's the difference?," [Online]. Available: https://www.3dhubs.com/knowledge-base/pla-vs-abs-whats-difference.

[38] schlotzz, "Compact Bowden Extruder, direct drive 1.75mm," [Online]. Available: https://www.thingiverse.com/thing:275593. [Accessed 6 11 2017].

[39] T. W. J. I. T. K. a. N. E. C. Schneider, "Characterisation of interface of steel/magnesium FSW," *Science and Technology of Welding and Joining,* vol. 16, pp. 100-105, 2011.

[40] G. H. A. B. T. R. W. J. B. C. S. K. C. B. Telma Blanco Matias, "Processing and characterization of amorphous magnesium based alloy for application in biomedical implants," *Journal of Materials Research and Technology,* vol. 3, no. 3, pp. 204-209, September 2013.

[41] Ultimaker, "Cura 2.7 download website," [Online]. Available: https://ultimaker.com/en/products/cura-software/list. [Accessed 6 11 2017].